Polymer Chemistry

ROYAL SOCIETY OF CHEMISTRY

PAPER

View Article Online
View Journal | View Issue

Cite this: *Polym. Chem.*, 2022, **13**, 1844

Optically reconfigurable shape memory metallopolymer mediated by a carbolong complex and radically exchangeable covalent bond†

Liulin Yang,‡[a] Haibo Zhao,‡[a] Yulin Xie,[a] Pufan Ouyang,[a] Yonghong Ruan,[a] Jiangxi Chen,[b] Wengui Weng,[a] Xumin He*[a] and Haiping Xia*[c]

Received 12th February 2022,
Accepted 3rd March 2022

DOI: 10.1039/d2py00192f

rsc.li/polymers

Conventional shape memory polymers (SMPs) are restricted to predetermined permanent shapes and therefore cannot be reconfigured arbitrarily to adapt to variant application scenarios. Meanwhile, shape memory behaviour is mostly thermally active and is often induced by direct heating and lacks spatial or remote control. Herein, we report a novel SMP with a reconfigurable network containing a semi-crystalline polymer chain, radically exchangeable covalent bond and photothermoresponsive carbolong complex moiety. The photothermal effect of the carbolong complex and the thermal responsiveness of the semi-crystalline polymer chain and radically exchangeable covalent bond lead to shape memory behaviour and network topological rearrangement using near-infrared light irradiation. Such a strategy offers an opportunity for building reconfigurable shape memory polymers that can be manipulated by either direct heating or remote light irradiation.

Introduction

Shape memory polymers (SMPs) are cross-linked polymer networks that are able to switch between a temporary shape and a permanent shape in response to an external stimulus.[1–4] SMPs are anticipated to be applied in the fields of biomedical devices,[10] aerospace industry,[11] actuators,[12] flexible electronics[13] and so on. Although shape-memory polymers have been known for decades, growing interest in recent years has immensely pushed forward the development of SMPs, such as multi-shape memory,[5,6] reversible shape-memory,[7,8] and rapid shape-memory materials.[9]

Conventional SMPs often have 'permanent' shapes immobilized that are hard to meet the demand of complex geometries for practical applications. The emergence of thermadapt polymer networks,[14] achieved *via* dynamic covalent bond exchanges, offers an ideal solution to tackle this problem.[15–19] The integration of thermal plasticity allows SMPs to reconfigure the permanent shape in an almost unrestricted manner. Therefore, the 'permanent' shapes are not limited by the initial moulding techniques. Up to now, a great variety of dynamic covalent bonds have been adopted to achieve thermal plasticity in polymer networks and/or thermadapt SMPs, such as disulfide bonds,[20] Diels–Alder moieties,[19,31] hydroxyl-esters,[21,22] urethanes,[17,23] imines,[24] C–N bonds,[25] boronic esters,[26] and radically exchangeable covalent bonds.[27–30] Radically exchangeable covalent bonds are available with a variety of structures and exhibit different dynamic behaviours under various temperatures without catalysts and show great advantages towards the construction of thermadapt polymer networks and SMPs. We have reported the synthesis of a 2,2′-bis (2-phenylindan-l,3-dione) radically exchangeable covalent bond for the construction of dynamic polymer networks and SMPs.[32,33]

Both shape memory behaviour and dynamic bond exchange are mostly thermally active and are often triggered by direct heating that lacks spatial or remote control. Triggering through photothermal effect, especially near infrared (NIR) irradiation induced photothermal effect, characterized by remote spatio-temporal selectivity, large penetration depth, and less damage to the polymeric material, is anticipated to address this challenge. We speculate that a synergistic combination of shape memory, thermal plasticity and photothermal effect in a single SMP system may offer an opportunity to manipulate the shape memory and the network topological rearrangement of a polymer in a precise spatial and temporal controlled way.

To this end, we constructed a polyurethane-based SMP with a semi-crystalline polycaprolactone chain, radically exchangeable TEMPO-based alkoxyamine moiety whose thermal

[a]*College of Chemistry and Chemical Engineering, Xiamen University, Xiamen, China. E-mail: hejin@xmu.edu.cn*
[b]*Department of Material Science and Engineering, College of Materials, Xiamen University, Xiamen, China*
[c]*Shenzhen Grubbs Institute, Department of Chemistry, Southern University of Science and Technology, Shenzhen, 518055, China. E-mail: xiahp@sustech.edu.cn*

†Electronic supplementary information (ESI) available. See DOI: 10.1039/d2py00192f

‡These authors contributed equally.

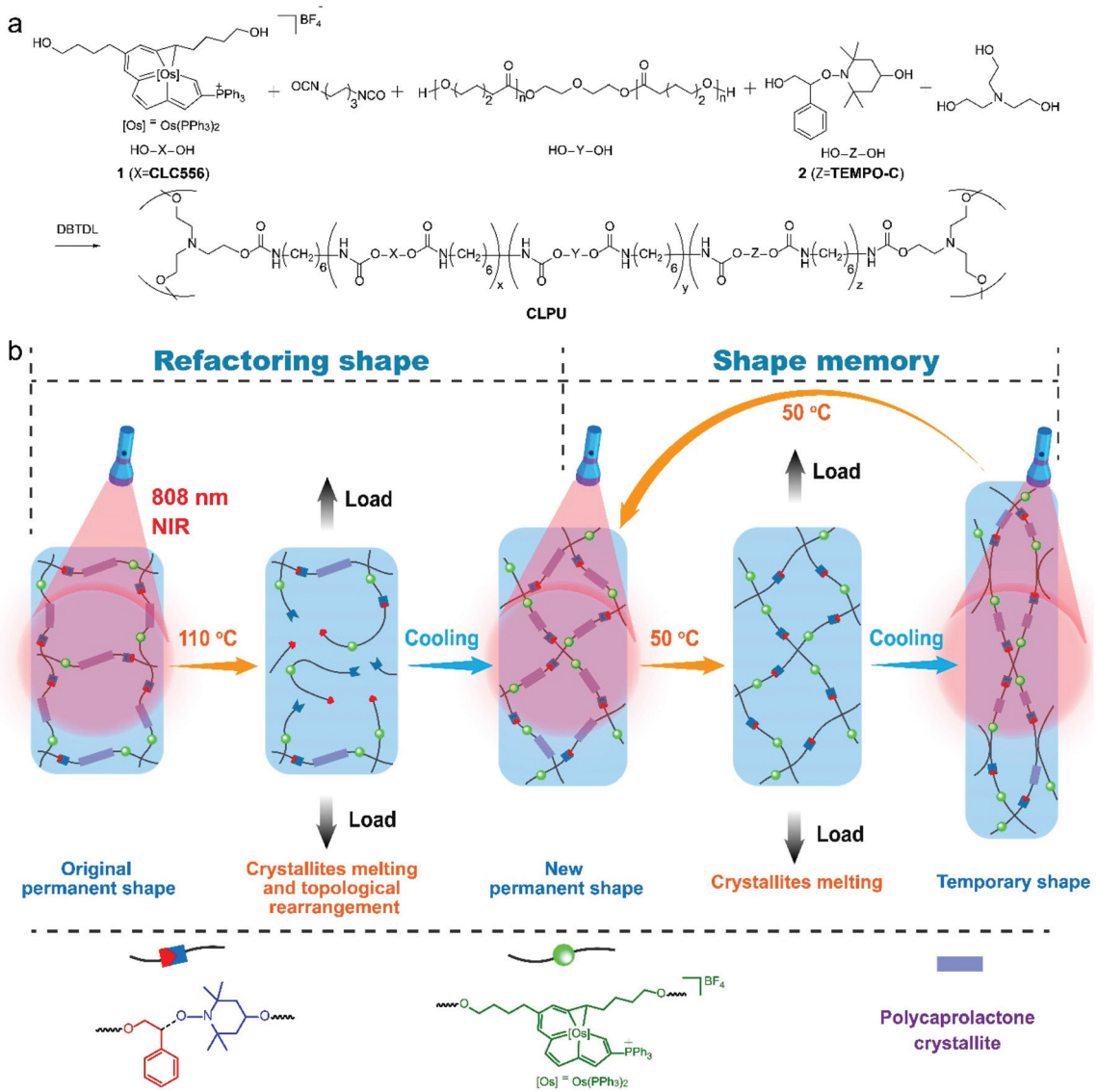

Scheme 1 (a) Synthesis of polymer network containing a semi-crystalline polycaprolactone chain, radically exchangeable TEMPO-based alkoxyamine covalent bonds and a photothermoresponsive carbolong complex moiety. (b) Schematic illustration of the optically reconfigurable shape memory of the polymer network.

exchange is tolerant of many functional groups[34] and an integrated photothermally responsive carbolong complex moiety (Scheme 1a). Taking advantage of the photothermal effect of the carbolong complex and the thermal responsiveness of the semi-crystalline polymer chain and the radically exchangeable covalent bond, we were able to manipulate the shape memory behaviour and network topological rearrangement using near infrared light irradiation (Scheme 1b).

Results and discussion

Synthesis of polymer networks

The carbolong complex (denoted **CLC556**, Scheme 1a) used here is a metal bridgehead polycyclic framework featuring a long carbon chain (≥7C) coordinated to a metal *via* metal–carbon bonds[35,36] and has been demonstrated to be an excellent NIR-responsive photothermal conversion moiety.[37–42] The hydroxyl functionalized carbolong complex compound **1** was synthesized according to the published procedure.[37] 1-(2-Hydroxy-1-phenylethoxy)-2,2,6,6-tetramethylpiperidin-4-ol (compound **2**), containing a radically exchangeable TEMPO-based alkoxyamine moiety (denoted **TEMPO-C**), was synthesized in two steps from commercially available materials (Scheme S1†).[43] A polyurethane-based network (**CLPU1**) containing a carbolong complex, a **TEMPO-C** and a polycaprolactone chain was readily synthesized *via* a two-step condensation polymerization protocol (Scheme 1a and ESI†). Two control polymer networks, one containing the carbolong complex but not **TEMPO-C** (**CLPU2**) and the other containing neither the

carbolong complex nor a **TEMPO-C** (**CLPU3**), were also prepared. The details of the polymer synthesis were elaborated in the ESI.†

Photothermal effect of the polymer networks

The photothermal effect of the carbolong complex **CLC556** in the polymer matrix was studied *via* NIR laser irradiation (λ = 808 nm, 0.5 W cm^{-2}). The sample temperature was monitored by using a thermal imaging camera. For **CLPU1** and control **CLPU2**, the surface temperature was increased to over 100 °C in 30 s and can be maintained at around 110 °C (Fig. 1a, b, and c) for one hour without significant attenuation, suggesting the excellent photothermal conversion capability and stability of **CLC556** in the polymer network. This thermal stability can be attributed to the unique aromaticity of the carbolong complex. Indeed, when heated under air conditions, the carbolong complex compound **1** could survive up to 160 °C without significant decomposition, as little change in the molecular structure was detected by NMR. Not surprisingly, the control **CLPU3** without **CLC556** showed almost no temperature increase upon NIR laser irradiation (Fig. 1a and d). Taking advantage of the photothermal conversion capability and thermal stability, heating and cooling of **CLPU1** can be repeated for several cycles without visible attenuation (Fig. 1e) by switching on and off the NIR laser. Therefore, it is possible to manipulate the shape memory behaviour and topological rearrangement by using NIR in a spatiotemporal manner.

Dynamic properties of the polymer networks

We started by examining the thermal dissociation of the **TEMPO-C** moiety in compound **2** by using electron spin resonance (ESR) spectroscopy measurements. As shown in Fig. S6,† the ESR signals of compound **2** in DMF solution started to strengthen when heated above 50 °C. The signal was significantly enhanced as the temperature reached 110 °C, indicating the abundant dissociation of compound **2** at high temperatures. Such a temperature-dependent trait is in accordance with the generation of radicals.[27] **CLPU1** containing **TEMPO-C** was then examined by variable temperature ESR. The ESR signals as a function of temperature are shown in Fig. 2. It is clear that **TEMPO-C** also showed a thermal dissociation behaviour in the polymer network. It is worth noting that a significant increase in the ESR signal only occurs at around 100 °C, higher than that of compound **2** in the solution state. This can be due to the fact that **TEMPO-C** is less dynamic in the solid-state polymer network. Moreover, it can be deduced that significant dissociation of **TEMPO-C** occurs at higher temperatures than at the melting temperature of polycaprolactone crystallites (Fig. S8†). This temperature difference is suitable for the manipulation of shape memory based on the melting and crystallization of polycaprolactone and the rearrangement of its topological network structure due to the dissociation and reformation of **TEMPO-C** at different temperatures. By adjusting the power of the NIR laser, the photothermally induced temperature increase can be controlled at lower magnitudes. Therefore, we were able to manipulate both

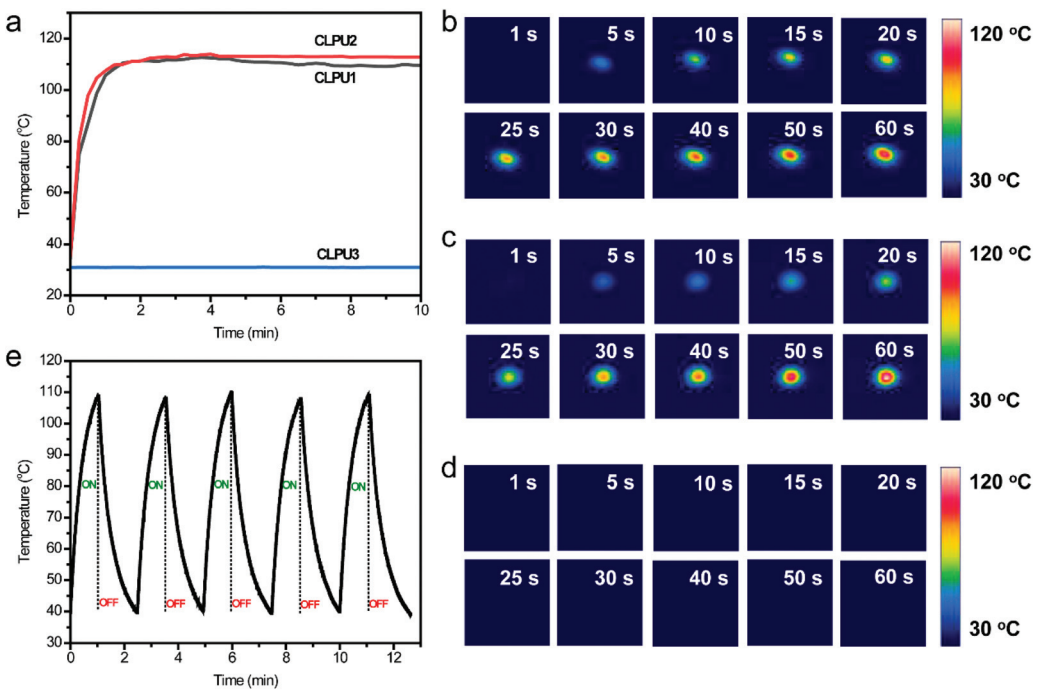

Fig. 1 (a) Surface temperature of polymer networks as a function of NIR laser (λ = 808 nm, 0.5 W cm^{-2}) irradiation time; infrared thermal images of irradiated spots from (b) **CLPU1**, (c) **CLPU2**, and (d) **CLPU3**; and (e) reversible light triggered heating and cooling cycles of **CLPU1**.

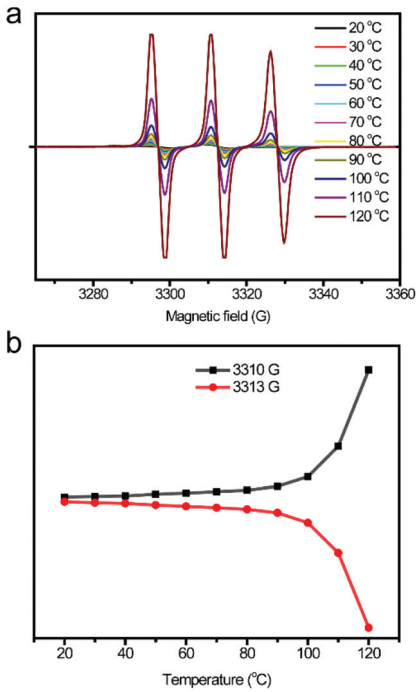

Fig. 2 (a) ESR spectra of **CLPU1** measured at variable temperatures; (b) ESR signals of **CLPU1** at 3310 G and 3313 G as a function of temperature.

shape memory and rearrangement of a topological network structure by NIR irradiation. Meanwhile, the carbolong complex **CLC556** has been verified to be stable at 110 °C, which guarantees the steady operation of the system.

The dynamic property of **CLPU1** was also verified by a swelling experiment. Two pieces of square **CLPU1** samples were soaked in DMF at room temperature (Fig. 3a) and 110 °C (Fig. 3b), respectively. After 30 min, the sample soaked at room temperature was swollen into an enlarged organic gel, similar to conventional covalent polymer networks. This phenomenon indicates that **CLPU1** is a covalent polymer network and the dynamic moieties in the network are stable at room temperature. However, the sample soaked at 110 °C was completely dissolved after 30 min, more like the behaviour of thermoplastic polymers. This unique behaviour can be ascribed to the dynamic bond breaking of **TEMPO-C** moieties in the polymer network at elevated temperatures.

The incorporation of dynamic covalent bonds can endow the polymer networks with unique stress relaxation and creep behaviours. Indeed, stress relaxation tests of **CLPU1** (Fig. 4a) showed that at relatively low temperatures (<50 °C), the stress declined quickly in the beginning and then relaxed very slowly, akin to that of the control **CLPU2** without **TEMPO-C**. When heated to 80 °C and above, the stresses of both **CLPU1** and **CLPU2** relaxed faster towards zero than when operated at lower temperatures. The relaxation was much slower for control **CLPU2** than **CLPU1** (80 °C and 110 °C). Such stress relaxation behaviours indicate that **CLPU1** is more like a conventional thermoset polymer at relatively low temperatures due to the slow dissociation of **TEMPO-C** and the melting of polycaprolactone crystallites (Fig. S7 and S8†). While at elevated temperatures, the significant dissociation of **TEMPO-C** led to the rearrangement of polymer segments to relax the stress faster. Besides the unique stress relaxation behaviours, the polymer network with **TEMPO-C** also showed a distinct creep behaviour compared to the control. The strain of sample **CLPU1** with a constant stress loading developed very slowly below 50 °C, which is again analogous to conventional thermoset polymers (Fig. 5a). However, the creep rate boosted dramatically when the sample was heated up to 110 °C, exhibiting plasticity as a result of the thermal dissociation of **TEMPO-C** in the network.

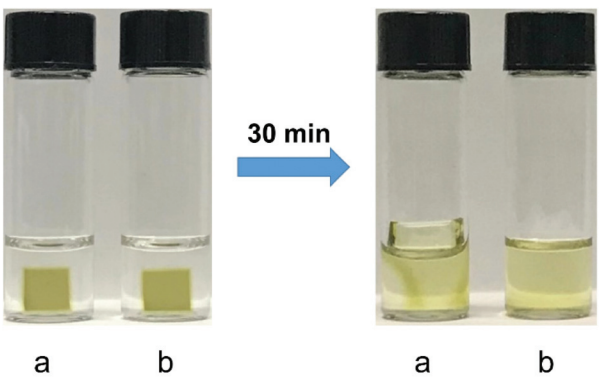

Fig. 3 Swelling behaviours of **CLPU1** in DMF at (a) room temperature and (b) 110 °C.

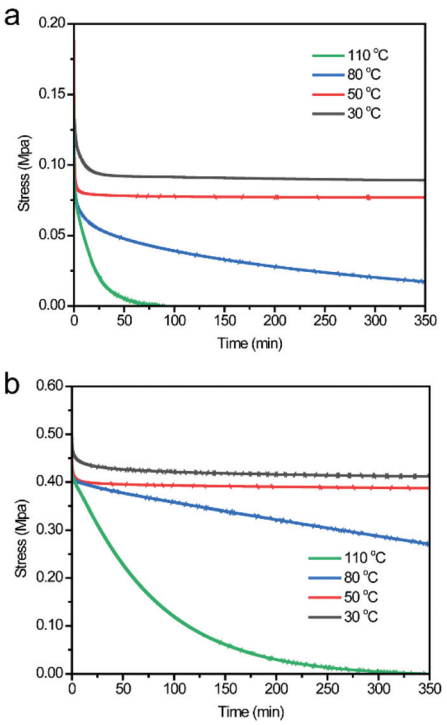

Fig. 4 Stress-relaxation curves of (a) **CLPU1** (b) **CLPU2** at variable temperatures.

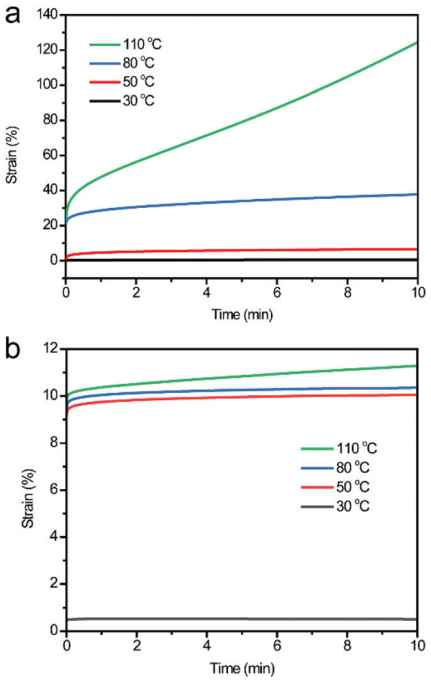

Fig. 5 Creep curves of (a) **CLPU1** (b) **CLPU2** at variable temperatures.

In contrast, **CLPU2** without **TEMPO-C** did not show such a dramatic creep rate change as temperature increased, despite the melting of polycaprolactone crystallites (Fig. 5b).

Shape memory and topological rearrangement of the polymer network

As demonstrated above, the melting of polycaprolactone crystallites occurs at a temperature lower than that for the significant thermal dissociation of **TEMPO-C** in the polymer network. Therefore, we were able to use the polycaprolactone crystallites as temporary crosslinks and their reversible melting-crystallization process to realize the shape memory behaviour.[18,44] When combined with the carbolong complex **CLC556** and its photothermal effect, the shape memory behaviour of the polymer network can be remotely controlled by NIR irradiation. As a demonstration, a rod-like **CLPU1** sample was stretched under NIR irradiation. The sample started to elongate when the temperature of the irradiated spot increased above 50 °C, owing to the melting of the polycaprolactone crystallites (Fig. S7 and S8†). When the sample was cooled down to room temperature after removing the NIR laser, the elongated shape of the sample was maintained owing to the crystallization of the polycaprolactone segments that froze the network temporarily. The sample was then hung on by using two clamps, and the shape memory behaviour was triggered by NIR irradiation. As shown in Fig. 6, upon NIR irradiation, the elongated sample contracted back to its initial length within a minute as evidenced by the lifting up of the lower clamp, indicating a relatively rapid one-way shape memory process. The strain–stress correlation during one-way shape memory of **CLPU1** was confirmed by a DMA test. As shown in Fig. 7, the sample was deformed when loaded with constant stress at 50 °C. The deformation was maintained when the temperature was decreased to −20 °C and the stress was removed successively. When the sample was heated up to 50 °C without stress loading, the shape of the sample returned to the initial state, indicating the shape memory behaviour of the sample. This process was repeated for six cycles and the shape memory property of the sample was mostly stable, although a slight permanent deformation was accumulated during these cycles. The accumulated permanent plastic deformation should be ascribed to the partial dissociation of dynamic **TEMPO-C** in the polymer network, which partially released the intrinsic stress of the sample and resulted in plastic deformation of the sample for each cycle (Fig. S9†).

Conventional shape memory materials are restricted by their predetermined initial shapes after processing, which

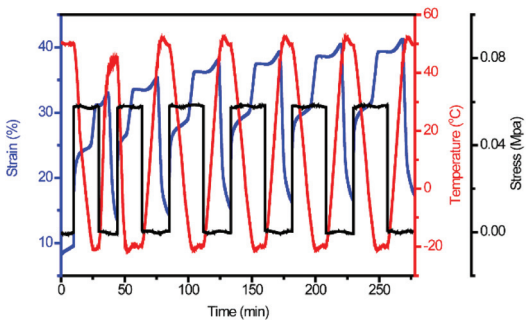

Fig. 7 DMA cycling tests for one-way shape memory of **CLPU1**.

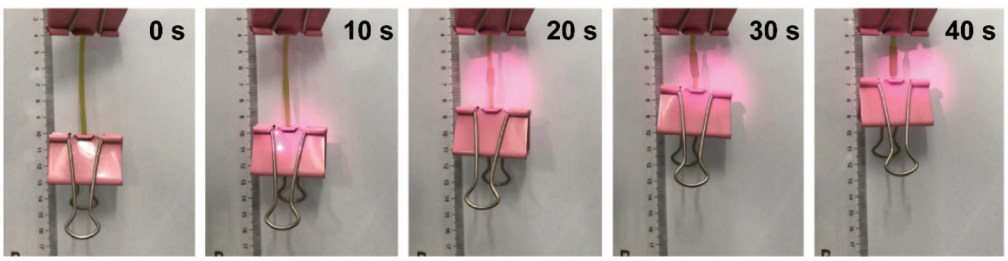

Fig. 6 One-way shape memory behaviour of **CLPU1**. The sample was first programmed into the temporary shape by stretching under NIR irradiation. No oxygen care was taken during this demonstration.

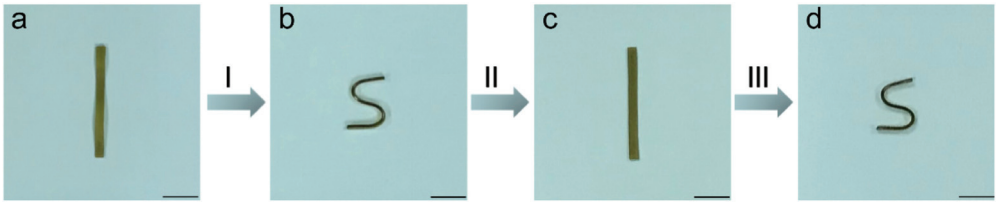

Fig. 8 Plastic shape memory of **CLPU1**. (a) Original permanent shape. (b) New permanent shape. (c) Temporary shape. (d) The temporary shape switched back to the new permanent shape. (I) The sample irradiated by NIR light and its temperature increased to 110 °C. (II) The sample was heated to 50 °C by NIR light. (III) The sample was heated to 50 °C by NIR light again. No oxygen care was taken during this demonstration.

cannot be reconfigured arbitrarily to adapt to various application scenarios.[16] A combination of plasticity and the shape memory property can overcome this limitation and make it possible to reset the permanent shape of the materials. In brief, a material goes through a designed plastic deformation under certain conditions and then the deformation is immobilized as a new permanent shape. The newly shaped sample can then perform a shape memory behaviour when triggered by a specific stimulus. To this end, our dynamic covalent **CLPU1** polymer network turns out to be an ideal candidate. As shown in Fig. 8, an "I" shape of the **CLPU1** sample was irradiated by NIR light for 1 h. During this period, the temperature of the sample was increased to 110 °C, thus dissociating the dynamic bonds from the moiety of **TEMPO-C**. Thereafter, the polymer was reconfigured into an "S" shape as the new permanent shape, on account of the plastic property of the sample under this condition. The new shape was then immobilized after removal of the irradiation and cooling down to reform the dynamic bonds. Next, the sample was reheated by NIR irradiation again, and the temperature of the sample was controlled to be 50 °C. While such a relatively low temperature can minimize the dissociation of the dynamic bonds, meanwhile, the melting of polycaprolactone crystallites was ensured. In this case, the sample can be programmed into a temporary "I" shape due to the melting and crystallization of polycaprolactone segments. When the sample was irradiated again, the new temporary "I" shape switched back to the permanent "S" shape, thus finishing one shape memory cycle. The plastic shape memory was also evidenced by the DMA test. As shown in Fig. 9, when the set temperature was lower than the dissociation temperature of the **TEMPO-C** moiety, the sample showed a typical one-way shape memory behaviour as demonstrated above. When the temperature was increased up to 110 °C, the **TEMPO-C** moiety dissociated and destroyed the polymeric network structure partially and temporarily. At this time, the sample was deformed by loading with transient stress. Such a deformation was maintained when the sample was cooled down, *i.e.* a new permanent shape was formed. Afterwards, when the same programming was applied again, the sample experienced a one-way shape memory process again on the basis of the new permanent shape, indicating a plastic shape memory behaviour.

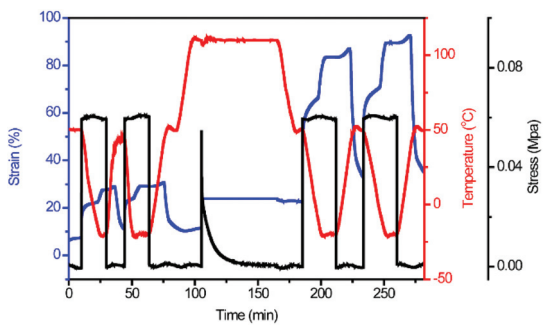

Fig. 9 DMA test for the plastic shape memory of **CLPU1**.

Conclusions

We have synthesized a novel polyurethane network with a semi-crystalline polycaprolactone chain, the photothermally responsive carbolong complex **CLC556** and a radically exchangeable dynamic **TEMPO-C** moiety. The radical dynamic covalent bond moiety endows polymer networks with dynamic property, while the photothermally responsive carbolong complex enables remote manipulation of the materials using NIR laser irradiation. Importantly, the combination of the photothermal effect of the carbolong complex, the thermal responsiveness of the semi-crystalline polymer chain and the radically exchangeable covalent bonds led to the reconfigurable shape memory behaviour that can be remotely controlled through NIR irradiation. We believe this line of research provides a general strategy to construct SMPs that can be manipulated in a precisely controlled way that is generally unrealized by conventional shape memory materials.

Experimental

General information

Polycaprolactone diol (M_n 2000) was purchased from J&K with vacuum drying before usage. Dibutyltin dilaurate (98%), 1,6-diisocyanatohexane (99%), 4-hydroxy-2,2,6,6-tetramethyl-piperidinooxy were purchased from Energy Chemical and used directly. Dichloromethane (AR) from Sinopharm was dried by CaH, styrene (95%) from Energy Chemical was purified by a basic Al_2O_3 column to remove the inhibitor, and benzoyl per-

oxide from Energy Chemical was dried by anhydrous Na_2SO_4. Argon (≥99.99%) from Linde Industrial Gases was used directly.

Tensile tests were carried out by using an Instron 3343 single-arm stretcher at a stretching rate of 5% of the initial length of the sample per second. The tensile tests were repeated three times for each sample for error analysis. The sample strip was 5.0 × 2.0 × 0.7 mm (length × width × thickness).

Nuclear magnetic resonance (NMR) spectra were recorded by using a Bruker Avance II 400 MHz, using tetramethyl silane (TMS) as an internal standard and deuterium methylene chloride as the solvent. Photothermal tests were performed by using an stl808t1-15w fiber coupling system and the data were collected by using a FLIR A35 FOV 24 thermal imager.

Differential scanning calorimetry (DSC) measurements were performed by using a DSC 240 F1 at a heating rate of 10 °C min^{-1} under N_2 atmosphere.

Optical images were taken by using an optical microscope (Guangzhou optical instrument factory), XDS-1 equipped with a 0.5 × CCD adapter.

X-ray powder diffraction (XRD) was performed by using a Rigaku Ultima-IV diffractometer with Cu Kα as the radiation source (λ = 0.154 nm).

Infrared spectra were recorded by using a Nicolet 380 Fourier transform infrared spectrometer, using KBr pellets.

Electronic spin resonance spectra were recorded by using a Bruker EMX-10/12 electronic spin resonance spectrometer.

Dynamic thermomechanical analysis was carried out by using a dynamic thermal mechanical analyser TA 850 at a test frequency of 1 Hz and a heating rate of 5 °C min^{-1} in N_2.

Stress relaxation tests were conducted by using a TA 850 dynamic thermal mechanical analyser. In stress relaxation tests, the sample was stretched for 1 mm first and then the length of the sample was maintained.

Creep tests were conducted by using a TA 850 dynamic thermal mechanical analyser. For creep tests, a stress of 0.1 N was applied on the sample for 10 min and then the stress was removed.

Synthesis of 2

Anhydrous benzoyl peroxide (0.63 g, 0.45 eq.), 4-hydroxy-2,2,6,6-tetramethyl piperidine oxygen (1.0 g, 1.0 eq.), and 20 mL of distilled styrene were mixed into a 50 mL round-bottom flask. The mixture was stirred at 90 °C under Ar for 24 h. Then the excess styrene was removed by distillation and the remaining mixture was dried by rotary evaporation. The crude product was purified by silica column (200–300 mesh) and eluted by petroleum ether (PE) : ethyl acetate (EA) = 3 : 1, resulting in a light yellow oily liquid (0.74 g, yield 36%). The light yellow oily liquid (1.00 g, 1 eq.) was dissolved in 20 mL of ethanol in a 50 mL round-bottom flask. Then, 2 mL of KOH (0.39 g, 2.8 eq.) aqueous solution was added to the flask. The solution was refluxed for 16 h, then ethanol was removed by rotary evaporation, and the residue was extracted using dichloromethane (30 mL) : water (30 mL) = 1 : 1 mixed solvent, which was followed by dichloromethane (30 mL × 2). The organic phase was then dried by anhydrous Na_2SO_4. After evaporation, the crude product was purified by a silica column (200–300 mesh), using petroleum ether : ethyl acetate = 1 : 1 as the eluent, to obtain compound **2** as a light yellow oil (0.59 g, yield 80%).

Table 1 Polymer networks synthesized with different feed ratios of **1** and **2**

Samples	Carbolong complex **1** (eq.)	Compound **2** (eq.)
CLPU1	0.14	10
CLPU2	0.14	0
CLPU3	0	0

Synthesis of polymer networks

A series of polyurethane samples were synthesized as shown in Table 1. Taking **CLPU1** as an example, the general synthesis route was: polycaprolactone (1.00 g, 20 eq.), compound **1** (5 mg, 0.14 eq.), and compound **2** (73.3 mg, 10 eq.) were added into a 50 mL round-bottom flask under N_2. Super dry dichloromethane (5 mL) and 1,6-diisocyanate (215 uL, 53.5 eq.) were then added to the flask. Polymerization was carried out at 30 °C for 4 h and then triethanolamine (30 uL, 9 eq.) was added. After crosslinking for 2 h, the mixture was poured into a PTFE mold, and then dried under 30 °C to obtain the crosslinked polyurethane film with a thickness of 0.7 mm.

Conflicts of interest

There are no conflicts to declare.

Acknowledgements

This work is supported by the Natural Science Foundation of China (No. 21931002 and 92156021), the Shenzhen Science and Technology Innovation Committee (no. JCYJ20200109140812302), and the Guangdong Provincial Key Laboratory of Catalysis (no. 2020B121201002).

References

1 Q. Zhao, H. J. Qi and T. Xie, *Prog. Polym. Sci.*, 2015, **49–50**, 79–120.
2 M. Behl, M. Y. Razzaq and A. Lendlein, *Adv. Mater.*, 2010, **22**, 3388–3410.
3 M. Behl, K. Kratz, J. Zotzmann, U. Nöchel and A. Lendlein, *Adv. Mater.*, 2013, **25**, 4466–4469.
4 R. R. Kohlmeyer, P. R. Buskohl, J. R. Deneault, M. F. Durstock, R. A. Vaia and J. Chen, *Adv. Mater.*, 2014, **26**, 8114–8119.
5 T. Xie, *Nature*, 2010, **464**, 267.

6 N. Zheng, J. Hou, Y. Xu, Z. Fang, W. Zou, Q. Zhao and T. Xie, *ACS Macro Lett.*, 2017, **6**, 326–330.
7 L. F. Fan, M. Z. Rong, M. Q. Zhang and X. D. Chen, *J. Mater. Chem. A*, 2018, **6**, 16053–16063.
8 M. Zare, M. P. Prabhakaran, N. Parvin and S. Ramakrishna, *Chem. Eng. J.*, 2019, **374**, 706–720.
9 F. Guo, X. Zheng, C. Liang, Y. Jiang, Z. Xu, Z. Jiao, Y. Liu, H. T. Wang, H. Sun, L. Ma, W. Gao, A. Greiner, S. Agarwal and C. Gao, *ACS Nano*, 2019, **13**, 5549–5558.
10 W. Zhao, L. Liu, F. Zhang, J. Leng and Y. Liu, *Mater. Sci. Eng., C*, 2019, **97**, 864–883.
11 Y. Liu, H. Du, L. Liu and J. Leng, *Smart Mater. Struct.*, 2014, **23**, 23001.
12 F. Ge, X. Lu, J. Xiang, X. Tong and Y. Zhao, *Angew. Chem., Int. Ed.*, 2017, **56**, 6126–6130.
13 H. Gao, J. Li, F. Zhang, Y. Liu and J. Leng, *Mater. Horiz.*, 2019, **6**, 931–944.
14 N. Zheng, Y. Xu, Q. Zhao and T. Xie, *Chem. Rev.*, 2021, **121**, 1716–1745.
15 Z. Fang, N. Zheng, Q. Zhao and T. Xie, *ACS Appl. Mater. Interfaces*, 2017, **9**, 22077–22082.
16 L. Yang, G. Zhang, N. Zheng, Q. Zhao and T. Xie, *Angew. Chem.*, 2017, **129**, 12773–12776.
17 N. Zheng, Z. Fang, W. Zou, Q. Zhao and T. Xie, *Angew. Chem., Int. Ed.*, 2016, **55**, 11421–11425.
18 Q. Zhao, W. Zou, Y. Luo and T. Xie, *Sci. Adv.*, 2016, **2**, e1501297.
19 G. Zhang, Q. Zhao, L. Yang, W. Zou, X. Xi and T. Xie, *ACS Macro Lett.*, 2016, **5**, 805–808.
20 Y. Amamoto, H. Otsuka, A. Takahara and K. Matyjaszewski, *Adv. Mater.*, 2012, **24**, 3975–3980.
21 D. Montarnal, M. Capelot, F. Tournilhac and L. Leibler, *Science*, 2011, **334**, 965.
22 Z. Pei, Y. Yang, Q. Chen, Y. Wei and Y. Ji, *Adv. Mater.*, 2016, **28**, 156–160.
23 D. J. Fortman, J. P. Brutman, C. J. Cramer, M. A. Hillmyer and W. R. Dichtel, *J. Am. Chem. Soc.*, 2015, **137**, 14019–14022.
24 P. Taynton, K. Yu, R. K. Shoemaker, Y. Jin, H. J. Qi and W. Zhang, *Adv. Mater.*, 2014, **26**, 3938–3942.
25 M. M. Obadia, B. P. Mudraboyina, A. Serghei, D. Montarnal and E. Drockenmuller, *J. Am. Chem. Soc.*, 2015, **137**, 6078–6083.
26 W. A. Ogden and Z. Guan, *J. Am. Chem. Soc.*, 2018, **140**, 6217–6220.
27 Z. P. Zhang, M. Z. Rong and M. Q. Zhang, *Adv. Funct. Mater.*, 2018, **28**, 1706050.
28 A. Takahashi, R. Goseki and H. Otsuka, *Angew. Chem.*, 2017, **129**, 2048–2053.
29 K. Imato, M. Nishihara, T. Kanehara, Y. Amamoto, A. Takahara and H. Otsuka, *Angew. Chem., Int. Ed.*, 2012, **51**, 1138–1142.
30 T. F. Scott, A. D. Schneider, W. D. Cook and C. N. Bowman, *Science*, 2005, **308**, 1615–1617.
31 G. Zhang, W. Peng, J. Wu, Q. Zhao and T. Xie, *Nat. Commun.*, 2018, **9**, 4002.
32 Y. Chen, L. Yang, W. Zheng, P. Ouyang, H. Zhang, Y. Ruan, W. Weng, X. He and H. Xia, *ACS Macro Lett.*, 2020, **9**, 344–349.
33 L. Yang, P. Ouyang, Y. Chen, S. Xiang, Y. Ruan, W. Weng, X. He and H. Xia, *Giant*, 2021, **8**, 100069.
34 T. Maeda, H. Otsuka and A. I. Takahara, *Prog. Polym. Sci.*, 2009, **34**, 581–604.
35 C. Zhu and H. Xia, *Acc. Chem. Res.*, 2018, **51**, 1691–1700.
36 D. Chen, Y. Hua and H. Xia, *Chem. Rev.*, 2020, **120**, 12994.
37 H. Zhang, H. Zhao, K. Zhuo, Y. Hua, J. Chen, X. He, W. Weng and H. Xia, *Polym. Chem.*, 2019, **10**, 386–394.
38 X. Lin, W. Xie, Q. Lin, Y. Cai, Y. Hua, J. Lin, G. He and J. Chen, *Polym. Chem.*, 2021, **12**, 3375.
39 Z. Lu, Q. Lin, Y. Cai, S. Chen, J. Chen, W. Wu, X. He and H. Xia, *ACS Macro Lett.*, 2018, **7**, 1034.
40 Z. Lu, Y. Cai, Y. Wei, Q. Lin, J. Chen, X. He, S. Li, W. Wu and H. Xia, *Polym. Chem.*, 2018, **9**, 2092.
41 Q. Lin, S. Li, J. Lin, M. Chen, Z. Lu, C. Tang, Z. Chen, X. He, J. Chen and H. Xia, *Chem. – Eur. J.*, 2018, **24**, 8375.
42 X. He, X. He, S. Li, K. Zhuo, W. Qin, S. Dong, J. Chen, L. Ren, G. Liu and H. Xia, *Polym. Chem.*, 2017, **8**, 3674.
43 W. Zou, J. Dong, Y. Luo, Q. Zhao and T. Xie, *Adv. Mater.*, 2017, **29**, 1606100.
44 T. Defize, R. Riva, J. Thomassin, M. Alexandre, N. V. Herck, F. D. Prez and C. Jérôme, *Macromol. Rapid Commun.*, 2017, **38**, 1600517.